Brazilian Journal of Chemical Engineering (2020) 37:351–368
https://doi.org/10.1007/s43153-020-00027-9

ORIGINAL PAPER

Biodiesel production from rubber seed oil using calcined eggshells impregnated with Al_2O_3 as heterogeneous catalyst: A comparative study of RSM and ANN optimization

Sai Bharadwaj Aryasomayajula Venkata Satya Lakshmi[1] · **Niju Subramania Pillai**[2] · **Meera Sheriffa Begum Khadhar Mohamed**[1] · **Anantharaman Narayanan**[1]

Received: 12 April 2019 / Revised: 23 July 2019 / Accepted: 24 July 2019 / Published online: 28 February 2020

Abstract

Experimental parameters influencing the transesterification of rubber seed oil (RSO) to biodiesel using alumina (Al_2O_3) impregnated on calcined eggshells (Al_2O_3/calcined eggshells) were studied in the present work. Parameters were optimized using response surface methodology (RSM) and artificial neural network (ANN). A conversion of 98.9% was observed for RSO at optimum conditions of 12:1 methanol: oil molar ratio, 3 (wt%) catalyst concentration and 4 (h) of reaction time. A significant quadratic model with molar ratio as the most influencing process parameter and a coefficient of determination, R^2, of value equal to 0.9379 is observed from RSM analysis. Best validation performance of 5.8595 at epoch-1 and R^2 value equal to 0.9740 was observed from ANN modeling. On comparing RSM and ANN models, it is concluded that ANN is a better tool for predicting the conversion of RSO to biodiesel with minimum error.

Graphic abstract

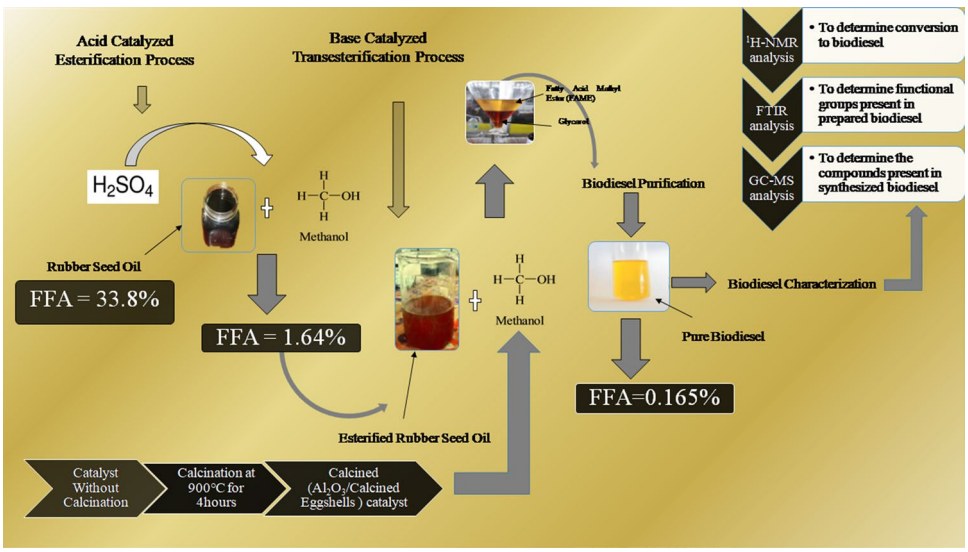

Keywords Artificial neural network · Biodiesel · Response surface methodology · Transesterification · Rubber seed oil

✉ Anantharaman Narayanan
naraman@nitt.edu

Extended author information available on the last page of the article

Introduction

Fossil fuels cause not only ecological problems, but also result in environmental degradation (Poonam Singh and Anoop 2011). Demand for environmentally friendly fuels as an alternative to fossil fuel is growing day by day. Many research works propose biodiesel, which is sustainable and biodegradable, as one of the best alternatives to fossil fuel (Yong-Ming et al. 2015). Production of biodiesel can be done in various ways like transesterification (Cynthia and Lee 2013), pyrolysis (Jemaa et al. 2015), Fischer–Tropsch process (Leibbrandt et al. 2013) etc. Recent studies reported that biodiesel production by a transesterification process is a better process which gives more conversion. The reaction between triglycerides and alcohols to produce methyl esters in the presence of a catalyst is called transesterification (Vipin et al. 2016). Edible oils are the most commonly used commercial feedstock for biodiesel production by a transesterification process (Anuradha et al. 2014; Sirajuddin et al. 2015; Istadi et al. 2015; Mostafa et al. 2017; Pisitpong et al. 2014; van der Westhuizen and Walter 2018; Canan et al. 2009; Medeiros et al. 2018). Use of edible oils as feed stocks in the biodiesel production is not preferred due to its other commercial applications. High free fatty acid (FFA) non-edible oils which do not have much commercial application can also be used for production of biodiesel (Prabu and Anand 2015; Taufiq-Yap et al. 2011; Jaya et al. 2015; Fadjar and Shiro 2015; Sunil et al. 2013; Olubunmi and Folasegun 2014; Chandrasekaran et al. 2017; Bharadwaj et al. 2019; Sakdasri et al. 2017). Low cost rubber seed oil (RSO) is a non-edible oil which can be used to produce biodiesel economically when compared to other feedstocks. Large quantity of rubber trees is present in the southern part of India, which can produce up to 5000 tonnes of oil per year (Ramadhas et al. 2005). Rubber seeds and oil produced from it do not have any major applications in daily life and were generally used either as fuel or treated as a waste. Hence, the oil extracted can be used as a feedstock in biodiesel production. RSO is highly viscous in nature, and has high molecular weight when compared to conventional diesel (Ramadhas et al. 2005; Hussain et al. 2016). A high free fatty acid (FFA) content in the oil feedstock leads to soap formation during biodiesel production process by base-catalyzed transesterification. Under such circumstances, acid esterification is the only pre-treatment step used to reduce the FFA content to less than 2 (Thodinh et al. 2016). Sulphuric acid, hydrochloric acid, and sulphonic acids are the commonly used acid catalysts. Hence, the FFA content in the raw RSO has to be reduced so that it can be used for biodiesel preparation. Acid-catalyzed transesterification, base catalyzed transesterification, acid–base catalyzed transesterification and enzyme-catalyzed transesterification are the four different transesterification processes for biodiesel preparation. A review of the literature indicates that base-catalyzed transesterification is a well-known process when compared to the rest (Dipesh Kumar et al. 2018). A lot of work has been carried out using homogeneous catalysts derived from alkaline metals such as potassium hydroxide (Madhu et al. 2012; Martin et al. 2012) and sodium hydroxide (Ehsan and Chowdhury 2015; Efavi et al. 2018). More soap formation and separation of catalyst from the final product are the major disadvantages observed while using homogeneous base catalysts. Heterogeneous base catalysts derived from solid waste shells, alkaline and alkali earth metals are a better replacement over homogeneous catalysts in biodiesel production by a transesterification process (Syazwani et al. 2017; Niju et al. 2014a, b, c; Girish et al. 2013; Chouhan and Sarma 2011; Trisupakitti et al. 2018). Use of modified solid base heterogeneous catalysts in biodiesel production by the transesterification process has been attempted using various feedstocks in recent times and some of the selected catalysts are cited in the literature (Surbhi et al. 2011; Wang et al. 2013; Wenlei and Haitao 2006; Niju et al. 2014a; Anjana et al. 2016; Sneha et al. 2015).

A comparison of two design models, response surface methodology (RSM) and artificial neural networks (ANN), in biodiesel production from high viscous RSO using modified heterogeneous solid base Al_2O_3/eggshells as catalyst is the novel part of the present research work. Alumina's high specific surface area, stability and ease of availability are the main reasons for choosing alumina (Al_2O_3) for impregnation with eggshells as catalyst in the present study (da Costa Evangelista et al. 2016). Molar ratio, catalyst concentration and reaction time are the parameters considered in this study. The calcined catalyst was characterized using scanning electron microscope–elemental dispersive spectrum (SEM–EDS), X-ray diffraction (XRD), Fourier transform infrared spectroscopy (FTIR) analysis. design of experiments (DOE) software version 10 was used to prepare complete experimental design for biodiesel preparation (Junaid et al. 2014). The statistical tool RSM was used to determine the relationship between the experimental output and designed output. Computational model based on the functioning of a biological neural network, called an artificial neural network (ANN), was used in the present study (Olusegun and Modestus 2018). Comparison between RSM and ANN was done to identify the best model in the present work. Synthesized biodiesel was analyzed by Fourier transform infrared spectroscopy (FTIR), ^{1}H-NMR (nuclear magnetic resonance), and gas chromatography–mass spectrometry (GC–MS) techniques.

Materials and methods

Materials

RSO for the present study was purchased from Virudhunagar, Tamil nadu. Methanol (analytical grade) was supplied by M/s. CDH suppliers, New Delhi, India. Sulphuric acid (98% concentration, EMPARTA) and alumina (Al_2O_3) were supplied by Merck life sciences private limited, Mumbai. Eggshells were collected from a nearby restaurant in Trichy, Tamilnadu.

Methods

Catalyst preparation

Initially the eggshells were washed with double distilled water to remove dirt from them completely, and followed by drying at 105 °C in an oven. Fine powder of dried shells was prepared using a grinder, which is further subjected to calcination in a muffle furnace at 900 °C for 4 h to form calcium oxide.

In the second stage the alumina (Al_2O_3) was impregnated at a weight ratio of 0.25 with calcined eggshells (Al_2O_3/calcined eggshells) followed by oven drying for 24 h at 110 °C. The dried sample was subjected to recalcination at 900 °C for 4 h using a muffle furnace. The prepared catalyst was collected and stored in an air tight bottle to ensure that there was no addition of moisture into it and was used for all transesterification runs.

The reason for selecting a calcination temperature of 900 °C is that the calcium carbonate content present in the raw eggshells is converted to calcium oxide at the high calcination temperature of 900 °C (Niju et al. 2014b). Alumina (Al_2O_3) was selected for impregnation since it is a stable compound which can easily be synthesized from naturally occurring bauxite (da Costa Evangelista et al. 2016).

Catalyst characterization

Crystalline structure of the prepared catalyst was tested with an X-ray diffractometer (XRD) (Model: Ultima IV, Rigaku, Japan) using Cu Kα radiation. Elemental composition and surface morphology of the prepared catalyst were analyzed using scanning electron microscope–energy dispersive X-ray spectroscopy (SEM–EDS) (Model: S3000H, Hitachi, Japan). Identification of various functional groups present in the synthesized catalyst was analyzed using Fourier transform infrared spectroscopy (FTIR, Model: Perkin Elmer, Spectrum 2) analysis. Basicity of the catalyst was tested by using a Hammett indicator test.

Oil analysis

Physico-chemical characteristics and composition of the major fatty acids of raw rubber seed oil like acid number, viscosity, density, flash point, fire point were measured and compared with values in literature and are reported in Table 1. Acid value of the treated oil was calculated by titration (Niju et al. 2014c) and it was observed that the acid value of raw oil is higher when compared to the literature value, which indicates the presence of more free fatty acids in the feedstock. Presence of FFA in the oil will lead to by-product formation. The specific gravity bottle method was used for density measurement and the density of raw oil was found to be close to literature values. Viscosity of oil was measured using an Ostwald viscometer and was also high when compared to the values in the literature. Cleveland open cup apparatus was used for flash point and fire point determination (Niju et al. 2014a), and a gas chromatography–mass spectroscopic analyzer was used to determine the fatty acid composition of the raw oil. Both the values were in fair agreement with the reported literature values.

Table 1 Physico-chemical properties of raw oil

Property	Raw oil (present work)	References					
		Ramadhas et al. (2005)	Hussain et al. (2016)	Jolius et al. (2012)	Zamberi and Ani (2016)	Jilse et al. (2016)	Ahmad et al. (2016)
Fatty acid composition (%)							
1. Palmitic acid	11.82	10.2		10.29		10.2	10.29
2. Linoleic acid	32.74	39.6	–	58.5	–	39.6	58.5
3. Oleic acid	40.81	24.6		20.07		24.6	24.6
4. Stearic acid	13.25	8.7		8.68		8.7	8.7
Acid number (mg KOH/g oil)	67.6	34	34	35.14	78.9	82	35.140
Viscosity (mm^2/s)	65.98	66.2	36	–	32.90	59.77	4.640
Specific gravity	0.91	0.91	0.93	0.92	0.9248	0.91	0.92
Flash point (°C)	222	198	220	–	–	–	154.6
Fire point (°C)	238.67	–	–	–	–	–	–

Biodiesel preparation

Pre-treatment of raw oil

From the physico-chemical characteristics of the raw oil presented in Table 1, it is observed that the acid value of the feedstock is 67.6 mg KOH/g oil, which would lead to soap formation if used directly without pretreatment in the case of a base-catalyzed transesterification process. The other main parameters to be considered in biodiesel preparation are density and viscosity. From Table 1 it is clear that the feedstock selected for biodiesel production has a high viscosity of 65.98 mm^2/s and specific gravity of 0.91. Use of highly viscous and dense oils directly in the diesel engine leads to scanty fuel atomization, partial combustion, carbon deposition and engine fouling (Ramadhas et al. 2005). Initial pretreatment of raw oil called esterification is the only method to optimize these parameters to the standard limits of biodiesel, as shown in Table 6.

Acid pre-treatment of raw oil called esterification with methanol was done at a reaction temperature of 65 °C, which is maintained with the help of a constant temperature water bath in the presence of sulphuric acid (98% concentrated) as acid catalyst to bring down the FFA content to less than 2. The acid value of pre-treated oil decreased to 2.97 (mg KOH/g oil) at optimized reaction conditions of 15:1 methanol: oil molar ratio, 3 (vol%) acid catalyst, and 2 h of reaction time. Subsequently, for all the transesterification studies, esterified oil was prepared under these conditions.

Transesterification experiment

Biodiesel preparation from rubber seed oil using Al_2O_3/calcined eggshells was performed in a constant temperature water bath with temperature maintained at 65 °C. A 3-neck round bottom flask was placed in the water bath with two corner necks connected to condenser and thermometer and the centre neck connected to a mechanical stirrer used for mixing the solution. At first the treated oil was heated at methanol boiling point temperature for specific time to ensure that excess methanol present in it had evaporated. On the other side the prepared catalyst is mixed with methanol using a magnetic stirrer. The catalyst methanol solution is then transferred into the treated oil, and then the transesterification experiments are performed for all the design runs shown in Table 4. At the end of the reaction the final product was filtered using Whatman No. 1 filter paper and then transferred to a separating funnel to separate the catalyst and the product. After 2 days, two different layers called fatty acid methyl esters (FAME) and excess glycerol were visible in the separating funnel. The top FAME layer was drawn from the separating funnel and excess methanol was removed using a rotary evaporator, followed by characterization of prepared biodiesel (Niju et al. 2014b).

Biodiesel characterization

Conversion of synthesized biodiesel was analyzed using ^{1}H-nuclear magnetic resonance (NMR) (Model: Bruker 500 MHz) and was calculated using Eq. (1) given by Gerhard (2001). Fourier transform infrared (FTIR) spectroscopic analysis was used to find the presence of ester functional groups and gas chromatography–mass spectroscometric (GC–MS) analysis was done to determine the composition of the biodiesel prepared:

$$\text{Conversion}\% = \frac{2 \times A_{ME}}{3 \times A_{\alpha-CH_2}} \times 100, \quad (1)$$

where, A_{ME} is the integration value of methoxy protons of formed methyl esters and $A_{\alpha-CH_2}$ is the integration value of α-methylene protons of formed methyl esters.

Design of experiments

As per stoichiometry for the transesterification process, 3 mol of alcohol react with 1 mol of oil for biodiesel production (Chouhan and Sarma 2011). The overall design for the optimization of experimental parameters in biodiesel production was done through central composite design (CCD) using design expert 10 software. Based on the initial trial runs, the range of minimum and maximum coded values of process parameters for biodiesel production by transesterification are: molar ratio 6 (mol/mol) and 12 (mol/mol), catalyst 3 (wt%) and 5(wt%), and reaction time 2 (h) and 4 (h). Process variables with the range of coded factors for the complete process are shown in Table 2.

Response surface methodology (RSM)

Methanol:oil molar ratio (mol/mol), catalyst (wt%) and reaction time (h) are the three experimental parameters selected for optimization as shown in Table 2. A second

Table 2 Coded values of process parameters

Factor	Name	Units	Minimum	Maximum	Coded values	
A	Molar ratio	mol/mol	3	15	− 1.000 = 6	1.000 = 12
B	Catalyst	wt%	2	6	− 1.000 = 3	1.000 = 5
C	Time	h	1	5	− 1.000 = 2	1.000 = 4

order quadratic model was suggested initially to determine the predicted conversion, as shown in Eq. (2). The significance of the suggested model and the effect of the most influencing parameter can be explained by ANOVA (analysis of variance) analysis developed from RSM studies. A graphical explanation of process parameters and their effect on biodiesel conversion was explained through two dimensional contour plots and three dimensional plots obtained for the entire design:

$$M = N_0 + N_1[A] + N_2[B] + N_3[C] + N_{12}[AB] + N_{13}[AC] + N_{23}[BC] + N_{11}\left[A^2\right] + N_{22}\left[B^2\right] + N_{33}\left[C^2\right], \quad (2)$$

where, N_0 is the intercept; N_1, N_2, N_3, N_{11}, N_{22} and N_{33} are the linear and quadratic constant coefficients; and N_{12}, N_{13} and N_{23} are the interaction constant coefficients.

A, B and C are the process parameters shown in Table 2 with coded factors which are to be optimized.

Artificial neural network (ANN) modeling

Nonlinear behavior of process inputs in the production of the corresponding desired output was measured by an artificial neural network (ANN) modeling. In this study, feed-forward back-propagation ANN model using the neural network training tool (nntraintool) was developed using MATLAB2018a for process parameter optimization. The TRAINLM (Levenberg–Marquardt) algorithm with TANSIG transfer function was used in training the network, which consists of a single input layer with three different neurons, a hidden layer with neurons and a single node output layer. Methanol-to-oil molar ratio (mol/mol), catalyst (wt%) and reaction time (h) are the three different neurons of input layer presently used in the study. Development of a relationship between input and output layers of the network is the main function of neurons in the hidden layer. Collection of information from the input layer associated with suitable weight factors in the production of a desired output is the main objective of neurons present in the hidden layer of the neural network. The measured output of the first hidden layer acts as input to the next consecutive hidden layer and the process continues progressively like this to produce a well desired output of the complete network. Network training by adjusting the weights to minimize the pre-defined error measure called mean square error (MSE) using an algorithm for parameter optimization is the second step of ANN modeling. Network training was carried out by using a training data subset and the results were evaluated using the validation data subset. When the MSE of the complete network as calculated using Eq. (3) was satisfactory, the test data subset was used to assess the prediction capability (Katarina et al. 2013; Obie et al. 2015). 20 data points were used for modeling, out of which 70% were used for training, 15% for validation and 15% for testing. The epoch was set at 1000 (default). The performance of the ANN for biodiesel conversion optimization was observed by mean square error (MSE) and coefficient of determination R^2:

$$\text{MSE (Mean Square Error)} = \frac{1}{n}\left(\sum_{i=1}^{n}(X - Y)^2\right), \quad (3)$$

where X is the experimental output, Y is the predicted output, n is the total number of training data.

Result and discussions

Characterization of calcined catalyst

X-ray diffraction (XRD)

The XRD pattern of the prepared catalyst is shown in Fig. 1. From the figure it is clear that 2θ values of 32.39°, 37.54°, 54°, 64.32°, 67.51°, and 79.77° indicate the presence of CaO and the peaks observed at 2θ values of 32.39°, 37.54°, 43.55°, 47.31°, 52.76°, 64.32°, 67.51°, 68.43°, 79.77° confirm the presence of Al_2O_3. All the peaks observed in the present work match well with reference peaks taken from Xpert High Score plus software with reference codes of 98-003-4906 for CaO and 98-011-3791 for Al_2O_3, respectively.

The crystallite size of the synthesized catalyst is calculated using the Williamson–Hall (W–H) equation as shown in Eq. (4) (Mote et al. 2012):

$$\beta\text{Cos}\theta = C_{\in}\text{Sin}\theta + \frac{K\lambda}{L}, \quad (4)$$

where β is the full width at half maximum, and is represented for every diffraction angle 2θ obtained from XRD analysis as shown in Table 3, K is the shape factor = 0.9; λ is the wavelength of copper (Cu) K_α radiation = 1.54; C_ϵ is the strain component and L is the crystallite size.

Upon substituting the β and θ values in Eq. (4), the X-axis (βcosθ) and Y-axis (sinθ) of the W–H plot are calculated and shown in Table 3.

The plot between $\beta\text{Cos}\theta$ and $\text{Sin}\theta$ of Eq. (4) shows the W–H plot of the present study as shown in Fig. 2, from which the intercept calculated can be used to determine the crystallite size of prepared catalyst.

From Fig. 2, the intercept $\frac{K\lambda}{L}$ is found to be 0.0012 and slope C_ϵ is 4.65×10^{-3}.

On further calculation with the intercept value observed from the plot, the crystallite size (L) of the synthesized catalyst used in the present study is 0.115 µm.

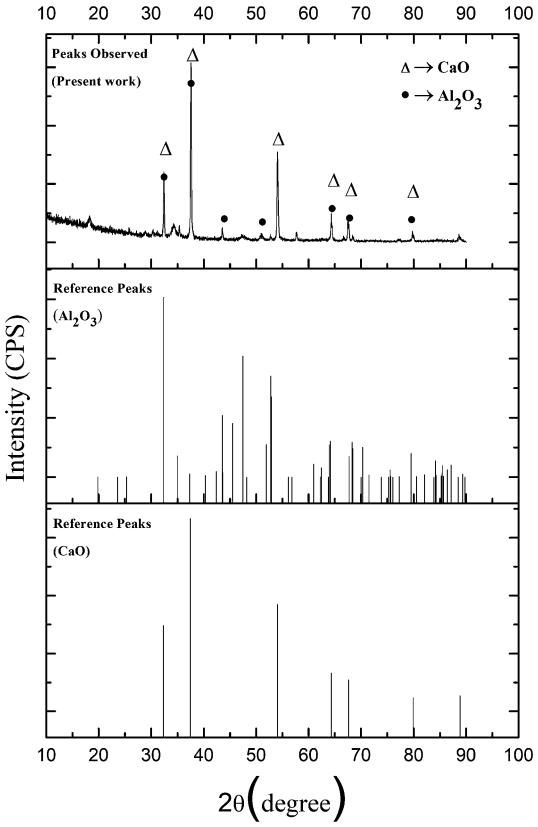

Fig. 1 X-ray diffraction (XRD) analysis of synthesized catalyst

Table 3 Complete details of the W–H plot

2θ	θ	B (radians)	X-axis (βcosθ)	Y-axis (sinθ)
32.39	16.195	2.0591×10^{-3}	0.278	0.00197
37.54	18.77	2.390×10^{-3}	0.321	0.00226
43.55	21.775	2.739×10^{-3}	0.370	0.00254
47.31	23.655	0.0109	0.401	0.00998
64.32	32.16	1.6752×10^{-3}	0.532	0.00141
67.51	33.755	2.739×10^{-3}	0.555	0.00227
68.43	34.215	5.4793×10^{-3}	0.562	0.00452
79.77	0.118	2.0591×10^{-3}	0.641	0.00158

SEM–EDS analysis

Scanning electron microscope (SEM) analysis of calcined catalyst before and after impregnation at different magnifications is shown in Fig. 3a calcined eggshells [(A) and (B)], Fig. 3b calcined impregnated catalyst (Al_2O_3/calcined eggshells) [(C) and (D)]. It is observed that various irregular rod type particles are found on the surface of catalysts before impregnation with Al_2O_3. For the catalyst after impregnation the shape of the particles changed to clustered lump shaped structures, which are due to recalcination of the impregnated

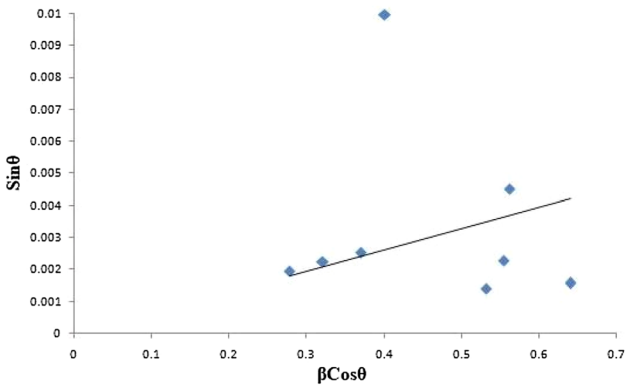

Fig. 2 Williamson–Hall plot of XRD analysis

catalyst at a higher temperature of 900 °C. Elemental dispersive spectroscopy (EDS) analysis of the calcined catalyst is presented in Table 4. From the table it is observed that 49.65 (wt%) of oxygen, 6.20 (wt%) of aluminum and 30.73 (wt%) of calcium are present, which indicate the presence of Al_2O_3 and CaO in the calcined catalyst. Lesser quantities of magnesium, carbon and other elements were also observed in the prepared catalyst.

Fourier transform infrared (FTIR) spectroscopy analysis of synthesized catalyst

An effective comparison of different functional groups present in the synthesized catalyst before and after impregnation was done by using Fourier transform infrared (FTIR) spectroscopic analysis as shown in Fig. 4. Sharp stretching peaks at wavenumbers 3600 cm^{-1} and 1100 cm^{-1} were observed in the catalyst before and after impregnation, which are due to the presence of hydroxyl groups with O–H bend vibrations attached to Al_2O_3 and CaO, which indicates the interaction between both the compounds. After complete decomposition of calcium carbonate present in the raw shell used for the synthesized catalyst, calcium oxide (CaO) formation was confirmed at wavenumbers between 1500 and 2000 cm^{-1} before impregnation, which is due to the presence of strong vibration of the O–Ca–O group with carbonate ions CO_3^{2-}, whereas the same is found with small vibrations in the range between 1500 and 2000 cm^{-1} for the catalyst after impregnation. The presence of Al–O bonds is observed at the wavenumber of 800 cm^{-1} after impregnation. The above functional groups observed indicate the presence of both Al_2O_3 and CaO.

Hammett indicator test

Basicity of the prepared catalyst was determined by the Hammett indicator test using phenolphthalein ($pK_a = 9.8$), indigo carmine ($pK_a = 12.2$) and 2,4-dinitroaniline

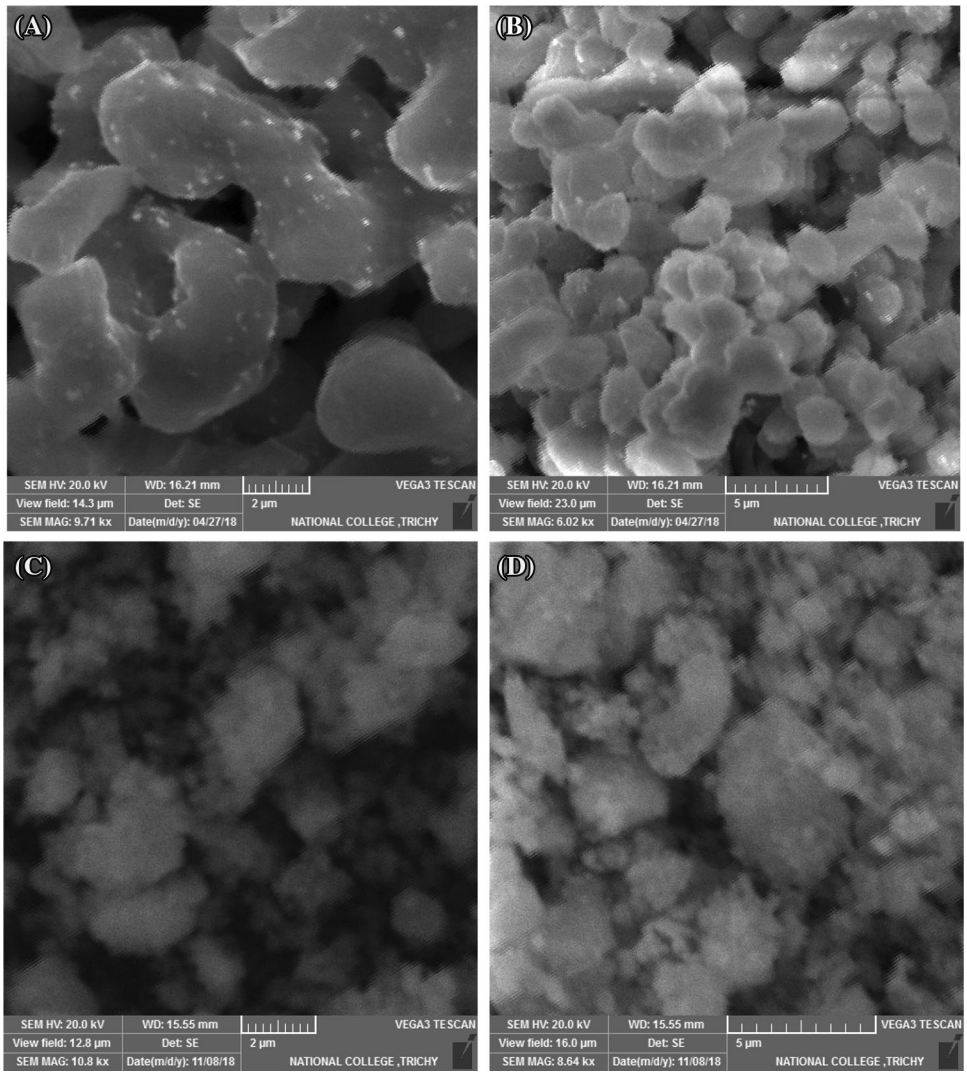

Fig. 3 SEM images of the catalyst: **a** and **b** calcined eggshells; **c** and **d** calcined impregnated catalyst (Al_2O_3/calcined eggshells)

Table 4 EDS analysis of the calcined catalyst

Element	Weight%	Atomic%
O	49.65	59.64
Al	6.20	4.41
Ca	30.73	14.74
Mg	0.33	0.26
C	13.10	20.96
Total	100.00	

($pK_a = 15$) as Hammett indicators. A pinch of the Hammett indicator was added to the catalyst-methanol solution and kept aside to equilibrate for 2 h. Strong basic nature of the catalyst can be identified for the solution in which an immediate colour change takes place, whereas for weak basic strength the solution does not show any colour change. In the present study, the basicity range of Al_2O_3/eggshells is observed as $12.2 < pK_a < 15$.

Optimization and modeling of biodiesel formed

Response surface methodology (RSM)

Transesterification experiments were designed using design expert software 10.0 based on central composite design (CCD) and are presented in Table 5. ANOVA analysis is reported in Table 6; from which it is observed that molar ratio, with a p value < 0.0001, is the most significant process parameter in the complete design. The second order quadratic model obtained is shown in Eq. (3), for predicting the biodiesel conversion for the entire design and is found to be significant with a p value < 0.0001. The F value of the model, which explains model efficiency and output response variance, is observed to be 16.78. The greater the F value, the greater the effect of that particular process parameter on the output. From the ANOVA analysis it is clear that methanol:oil molar ratio is the most significant process parameter affecting the biodiesel

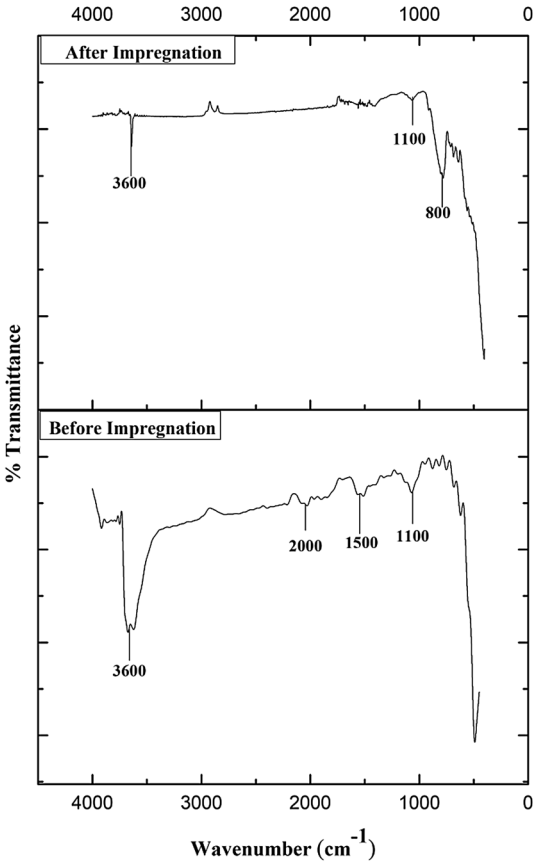

Fig. 4 FTIR analysis of calcined Al_2O_3/eggshells catalyst

conversion. Positive significance of the predicted output values can be explained by the coefficient of determination R^2 value, which is observed to be 0.9379. This shows that design using the RSM model is moderately good. The complete design equation in terms of actual parameters which are used to calculate the predicted conversion is given in Eq. (5):

$$\begin{aligned}\text{Conversion}\% = {} & 0.12432 + 13.424 \times (\text{Methanol} : \text{Oil}) \\ & + 1.92369 \times (\text{Catalyst}) + 6.49449 \\ & \times (\text{Time}) - 0.65208 \times ((\text{Methanol} : \text{Oil}) \\ & \times(\text{Catalyst})) - 0.52292 \times ((\text{Methanol} : \text{Oil}) \\ & \times(\text{Time})) - 0.95125 \times ((\text{Catalyst}) \times (\text{Time})) \\ & - 0.37780 \times (\text{Methanol} : \text{Oil})^2 + 1.07602 \\ & \times (\text{Catalyst})^2 + 0.46727 \times (\text{Time})^2 \end{aligned} \quad (5)$$

Effect of significant factor on synthesized biodiesel

ANOVA results of complete design conclude that methanol:oil molar ratio is the most significant process parameter, affecting the output. Based on the above results, two-dimensional contour plots and three-dimensional response plots for overall design are shown in Figs. 5 and 6, respectively. From these plots it is clear that, with an increase in the methanol:oil molar ratio (mol/mol) at constant catalyst concentration (Figs. 5a,6a) and constant reaction time (Figs. 5b,6b), the % conversion increases and reaches a maximum value. A further increase in molar ratio beyond this point results in a gradual decrease in % conversion, possibly due to the reversible action of the transesterification reaction. More methanol:oil ratio is needed while working with heterogeneous base catalysts in biodiesel production when compared to the use of homogeneous catalysts. High molar ratio of 18:1 is observed while using clam shells as heterogeneous catalysts in biodiesel production from waste cooking oil (Girish et al. 2013). 97.6% conversion to biodiesel was observed at molar ratio of 21:1 using a modified catalyst (Wei et al. 2015). Figures 5c and 6c show the variation in conversion as a function of catalyst concentration and reaction time for a constant methanol:oil molar ratio. From this plot it is observed that, with an increase in the catalyst concentration and reaction time, there is no significant change in conversion, which is attributed to the high activity of the prepared catalyst. A high conversion of 98.9% was observed at optimum parameters of 12:1 methanol:oil molar ratio, 3 (wt%) catalyst and 4 (h) of reaction time.

Artificial neural network (ANN) modeling

The complete neural network of an ANN model consisting of an input layer with three nodes, one hidden layer with 10 neurons and a single node output layer is considered in the present study (see Fig. 10 of the Appendix). Complete correlation between input and output layer can be explained by the coefficient of regression R value which is found to be good with values of 0.98716, 0.9779 and 0.99535 for training, validation and testing, respectively (see Fig. 11 of the Appendix). In training the network for several times, which is known as transformation of weights, a minimum error is observed between the predicted and experimental outputs for the complete design as shown in Table 5. The mean square error (MSE) value of 0.099405 for the overall design is calculated as per Eq. (3), with the best validation performance of 5.8595 at epoch-1 (see Figs. 12 and 13 of the Appendix).

Comparison of RSM and ANN

The experimental output and predicted output, based on the results is presented in Table 5 for both RSM and ANN and it is clear that a minimum error was observed between experimental output values and predicted output in the case of ANN when compared to values predicted by RSM (see Figs. 14 and 15 of the Appendix). Coefficients of determination, R^2 value, which explains the model competency, are found to be 0.9379 for RSM and 0.9740 for ANN. The root mean square error (RMSE) values for both RSM and ANN

Table 5 Complete design of transesterification experiments

Methanol: oil (mol/mol)	Catalyst (wt%)	Time (h)	Conversion% (experimental output)	Conversion% (RSM) (predicted output)	Conversion% (ANN) (predicted output)
9	4	3	89.19	89.92	88.17
9	2	3	87.91	90.61	88.98
9	6	3	95.92	97.85	96.09
6	3	2	74.6	73.66	72.71
9	4	1	89.18	90.22	88.79
9	4	3	89.18	89.92	88.16
12	5	2	98.51	96.99	97.00
9	4	5	89.78	93.37	93.38
9	4	3	89.19	89.92	88.16
6	5	2	84.56	83.09	84.68
12	3	4	98.9	95.72	99.45
9	4	3	89.19	89.92	88.16
3	4	3	60.29	61.64	60.79
12	5	4	97.23	93.53	96.50
9	4	3	89	89.92	88.16
6	5	4	87.73	85.90	84.05
12	3	2	98.2	95.38	94.87
9	4	3	89.19	89.92	88.16
6	3	4	83.4	80.27	84.18
15	4	3	87.73	91.00	89.14

Table 6 ANOVA analysis for conversion% optimization

Source	Sum of squares	df	Mean square	F value	p value prob > F	
Model	1379.15	9	153.24	16.78	< 0.0001	Significant
A-Methanol:oil	861.86	1	861.86	94.39	< 0.0001	Significant
B-Catalyst	52.38	1	52.38	5.74	0.0376	
C-Time	9.91	1	9.91	1.08	0.3221	
AB	30.62	1	30.62	3.35	0.0970	
AC	19.69	1	19.69	2.16	0.1727	
BC	7.24	1	7.24	0.79	0.3942	
A^2	290.69	1	290.69	31.84	0.0002	Significant
B^2	29.11	1	29.11	3.19	0.1045	
C^2	5.49	1	5.49	0.60	0.4560	
$R^2 = 0.9379$						

models for all the design experiments shown in Table 5 are calculated using Eq. (6) (Arpita et al. 2015), and the determined values are observed to be 2.136 for RSM and 1.649 for ANN. From the above results it is concluded that the ANN model is well suited when compared to RSM for predicting biodiesel production from RSO:

$$Root\ Mean\ Square\ Error(RMSE) = \sqrt{\frac{1}{n} \times [PO - EO]^2}, \quad (6)$$

where PO is the predicted output, EO is the experimental output, and n is the number of runs performed.

Characterization of the biodiesel formed

Physico-chemical properties of the prepared biodiesel

A comparison of various physico-chemical properties such as acid number, density, viscosity, and flashpoint of the prepared biodiesel with the values presented in the literature for biodiesel prepared from rubber seed oil using different catalysts is shown in Table 7. From this table, it is observed that all the properties of the synthesized biodiesel are well within the limits of ASTM standard values.

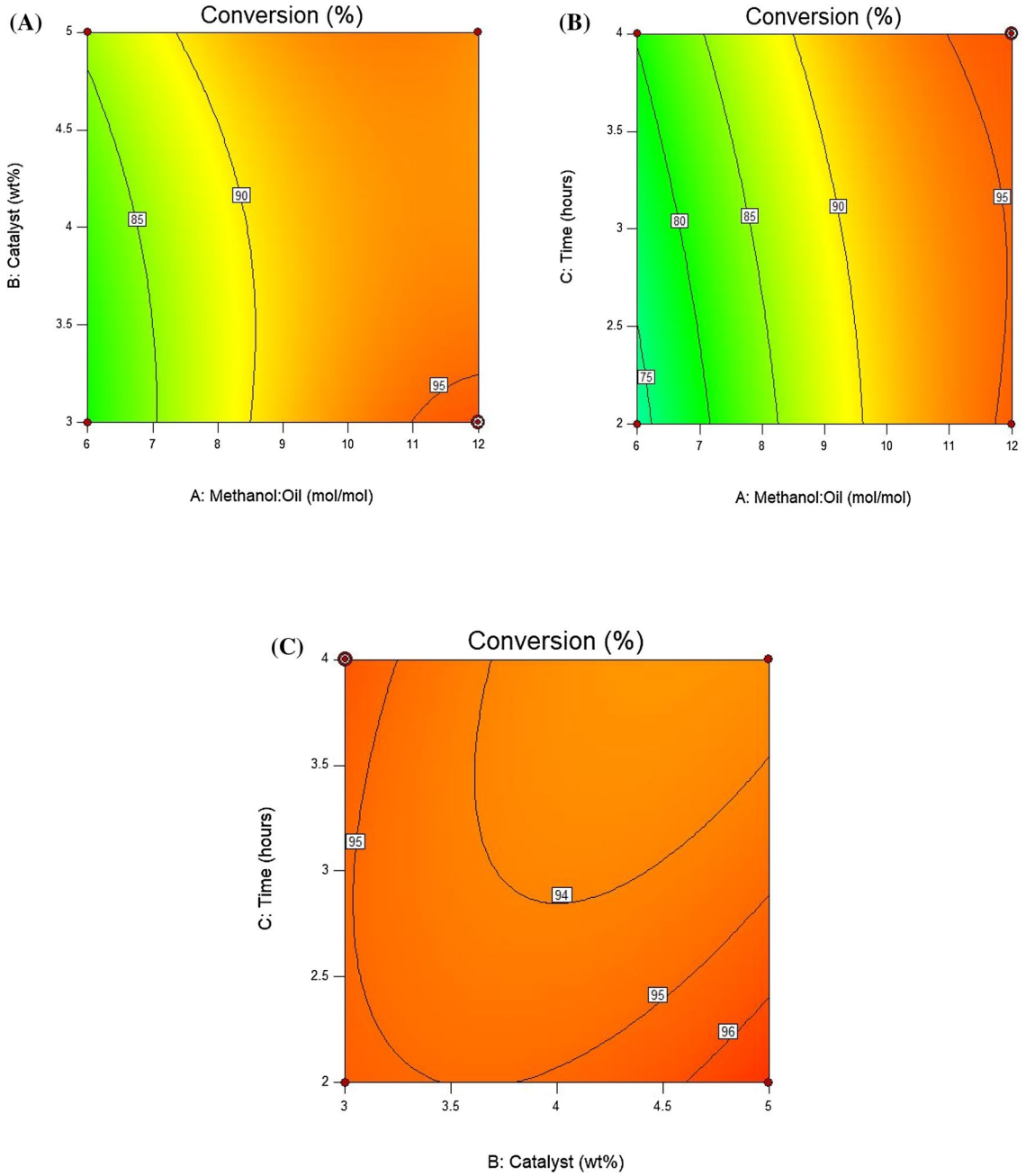

Fig. 5 Contour plots of conversion% response: [**a** molar ratio vs catalyst (wt%); **b** molar ratio vs time (h); **c** catalyst (wt%) vs time (h)]

^{1}H-Nuclear magnetic resonance (NMR) spectroscopic analysis

Conversion of RSO to biodiesel can be analyzed by ^{1}H-NMR spectroscopic analysis as shown in Fig. 7. Different peaks are observed in the figure, in which the presence of methoxy protons of methyl esters at 2.3 ppm and α-methylene protons of methyl esters at 3.6 ppm indicate the formation of biodiesel. Conversion of esterified oil to biodiesel was estimated using Eq. (1). At optimum conditions of 12:1 molar ratio (mol/mol), 3 (wt%) catalyst and reaction time of 4 h, a high conversion of 98.9% was observed. Table 8 shows comparison of biodiesel produced using the modified catalyst of the present research work with the other modified catalysts presented in the literature. From this table, it is concluded that conversion of RSO to biodiesel produced in this work is higher when compared to other works reported in literature.

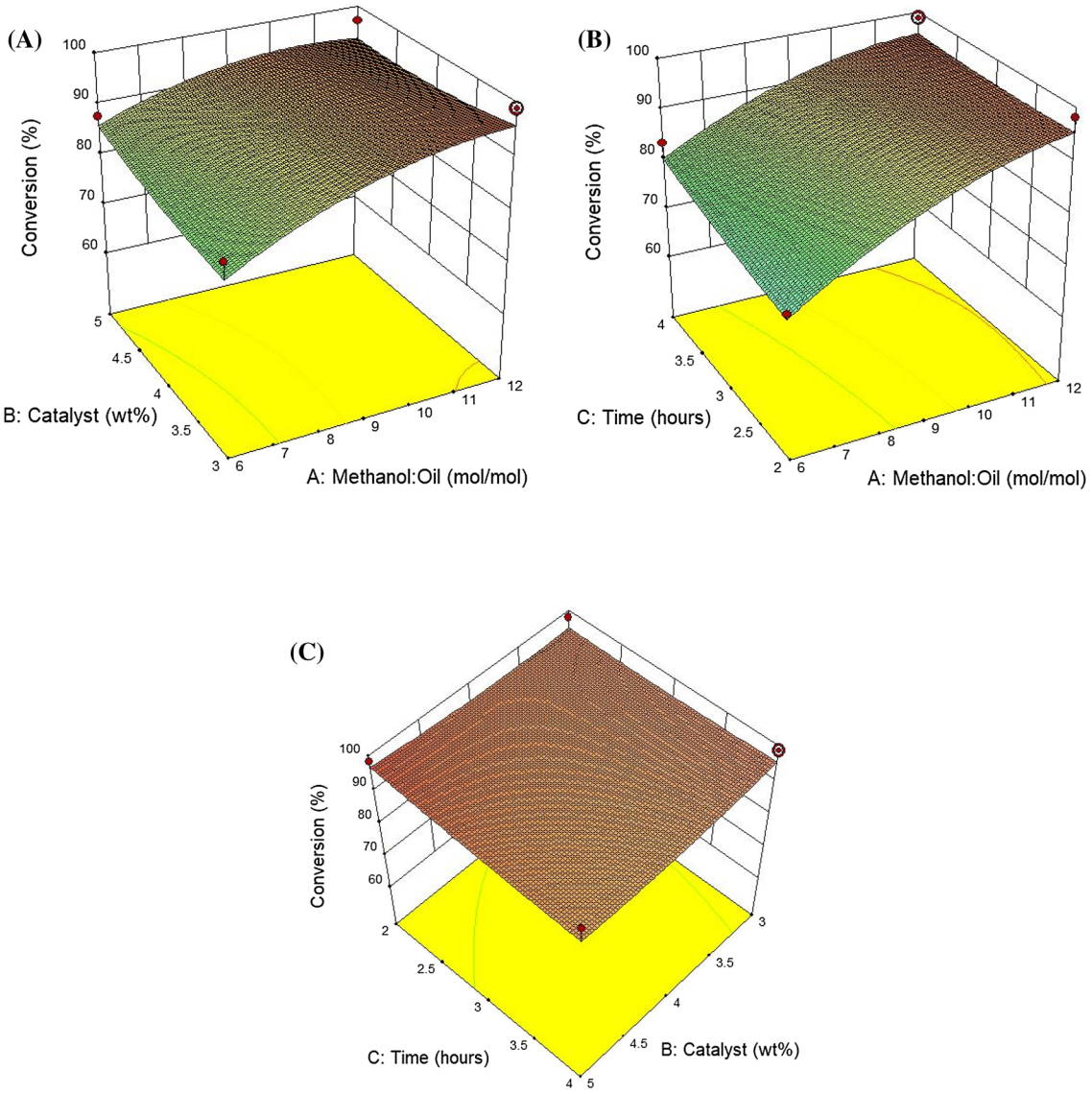

Fig. 6 3D plots of conversion% response [**a** molar ratio vs catalyst (wt%); **b** molar ratio vs time (h); **c** catalyst (wt%) vs time (h)]

Table 7 Physico-chemical properties of synthesized biodiesel

Properties	Acid value (mg KOH/g oil)	Specific gravity	Kinematic viscosity (mm^2/s)	Flash point (°C)
ASTM standard values	< 0.6	0.86–0.90	1.9–6.0	100–170
Present work	0.33	0.88	4.2	145
Mahbub et al. (2011)	0.12	0.85	4.5	120
Ikwuagwu et al. (2000)	0.9	0.885	6.29	235
Wuttichai et al. (2017)	0.35	0.80	4.84	184
Satyanarayana and Muraleedharan (2010)	–	0.871	4.98	164
Ru et al. (2011)	0.22	0.881	40.059	150
Melvin et al. (2011)	–	0.837	3.12	128

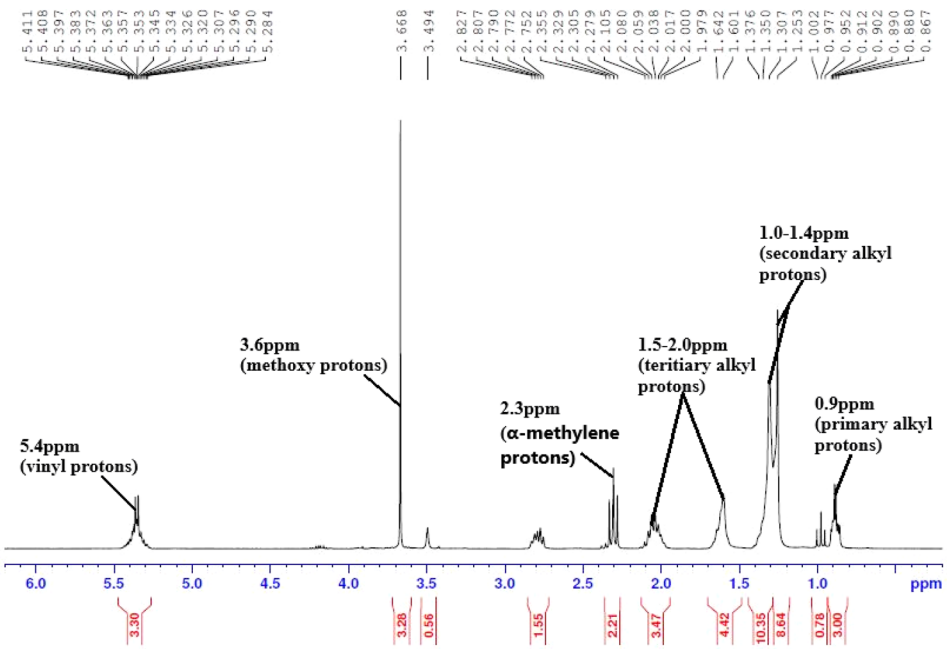

Fig. 7 ^{1}H-NMR analysis of prepared biodiesel

Table 8 Comparison of the prepared biodiesel with biodiesel prepared with other heterogeneous catalysts cited in the literature

Feedstock	Catalyst used	Conversion%	References
Soyabean oil	La/zeolite	48.9	Qing et al. (2007)
Soyabean oil	Mg/MCM-41	85	Georgogianni et al. (2009)
Soyabean oil	NaX zeolites loaded with KOH	85.6	Wenlei et al. (2007)
Jatropha oil	KNO_3/Al_2O_3	84	Amish et al. (2009)
Soyabean oil	$CaO–SnO_2$	89.3	Wenlei and Liangliang (2013)
Soyabean oil	WO_3 supported on $AlPO_4$	72.5	Wenlei and Dong (2012)
Rubber seed oil	Al_2O_3/calcined eggshells	98.9	Present work

Fourier transform infrared (FTIR) spectroscopic analysis of the synthesized biodiesel

Identification of ester functional groups present in the prepared biodiesel can be done only by Fourier transform infrared spectroscopy (FTIR) analysis and is shown in Fig. 8. The functional groups observed in the wavenumber range of 1744 to 730 cm^{-1} indicate the formation of ester compounds with different band stretch. Sharp peaks in the wavenumber range of 3009 to 2855 cm^{-1} indicate the presence of –C–H stretch. Table 9 shows the complete list of functional groups present the biodiesel.

Gas chromatography–mass spectrometry (GC–MS) analysis

GC–MS (TIC) analysis was performed with MS workstation 8 software equipped with 436-GC Bruker and TQ Quadrupole Mass Spectrometer, along with BR-5MS (5% diphenyl/95% dimethyl poly siloxane), 30 m × 0.25 mm ID × 0.25 µm df column to determine the composition

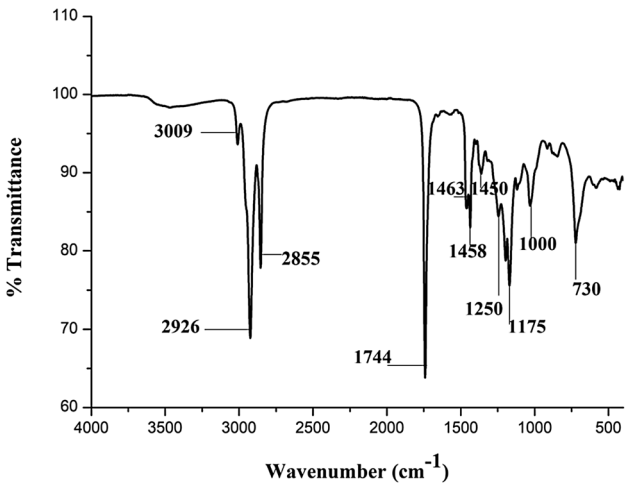

Fig. 8 FTIR analysis of prepared biodiesel

of prepared biodiesel. NIST Version-2011 is the library used for MS programme. Figure 9 shows the gas chromatogram of biodiesel produced from RSO, and Table 10 shows

Table 9 List of functional groups present in biodiesel

Wavenumber (cm^{-1})	Functional group
3009, 2926, 2855	–C–H stretch
1744, 1463, 1458 and 1450	Ester functional group with C=O stretch
1250, 1175 and 1000	Aliphatic esters with O=C–O–C stretch
730	S–OR esters

the list of compounds present in the prepared biodiesel. Close to 100% of biodiesel is formed with major amounts of dodecanoic acid methyl ester (19.27%), tetradecanoic acid methyl ester (19.59%), 9-hexadecenoic acid methyl ester (*Z*)- (19.48%), and hexadecanoic acid methyl ester (28.30%) present in it.

Conclusions

Application of a modified basic catalyst for biodiesel synthesis from highly viscous RSO has been studied. An effective comparison between two design models, response surface methodology (RSM) and artificial neural networks (ANN), is also discussed. Alumina (Al_2O_3) impregnated on calcined eggshells was used as heterogeneous catalyst, and the basicity of the prepared catalyst was found to be in the range of $12.2 < pK_a < 15$. Changes in the pore structure were observed on the surface of impregnated catalyst because of recalcination at the high temperature of 900 °C. A set of experimental runs was designed using design of experiments (DOE) software version 10 for RSM and ANN modeling. A high conversion of 98.9% was observed at the optimum conditions of 12:1 methanol: oil molar ratio (mol/mol), 3 (wt%) catalyst concentration and 4 h of reaction time. It is also concluded that, in the case of RSM analysis, the suggested quadratic model of the

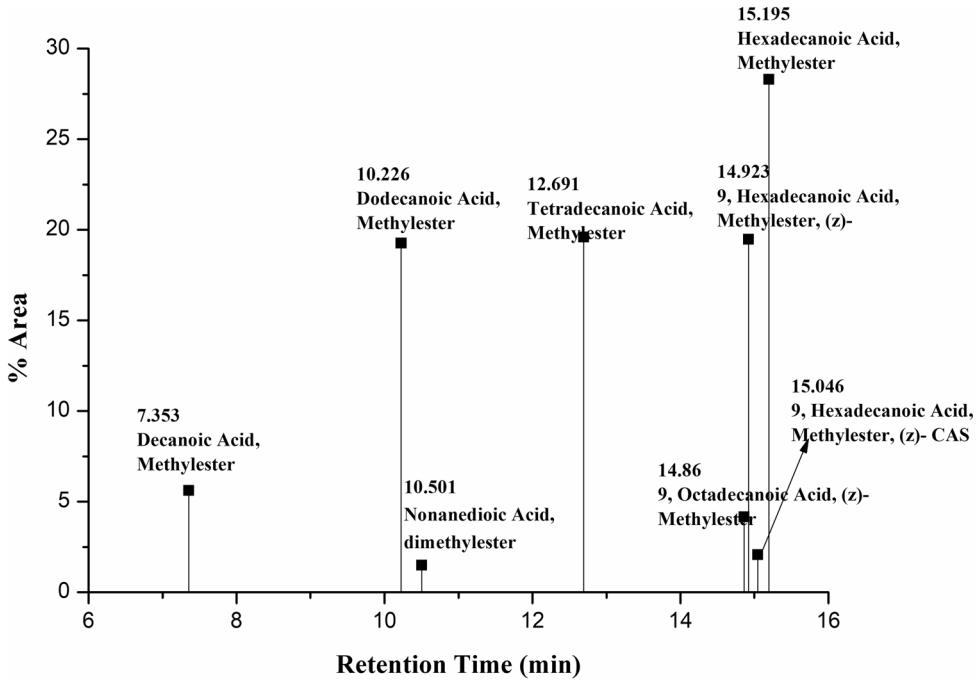

Fig. 9 GCMS analysis of the prepared biodiesel

Table 10 List of compounds identified in the prepared biodiesel

Retention time	Name of the compound	Molecular formula	Molecular weight	%
7.353	Decanoic acid, methyl ester	$C_{11}H_{22}O_2$	186	5.62
10.226	Dodecanoic acid, methyl ester	$C_{13}H_{26}O_2$	214	19.27
10.501	Nonanedioic acid, dimethyl ester	$C_{11}H_{22}O_4$	216	1.49
12.691	Tetradecanoic acid, methyl ester	$C_{15}H_{30}O_2$	242	19.59
14.860	9-Octadecenoic acid (*Z*)-, methyl ester	$C_{19}H_{36}O_2$	296	4.17
14.923	9-Hexadecenoic acid, methyl ester, (*Z*)-	$C_{17}H_{32}O_2$	268	19.48
15.046	9-Hexadecanoic acid methyl ester, (*Z*)-CAS	$C_{17}H_{32}O_2$	268	2.08
15.195	Hexadecanoic acid, methyl ester	$C_{17}H_{34}O_2$	270	28.30

complete design is significant, with methanol:oil molar ratio as the most influencing process parameter which affects the conversion of RSO to biodiesel. The mean square error (MSE) value of 0.099405 for the overall design with best validation performance of 5.8595 at epoch-1 was observed for ANN modeling. The coefficient of determination R^2 value, equal to 0.9379 was obtained by RSM, and a R^2 value of 0.9740, was obtained using the ANN model. The root mean square error (RMSE) of the models used were 2.136 for RSM and 1.649 for ANN, respectively. On comparing the above results for biodiesel production from RSO using Al_2O_3/calcined egg-shells as heterogeneous catalyst, it is concluded that the ANN model fits better, with minimum error, than RSM.

Compliance with ethical standards

Conflict of interest There are no potential conflicts of interest between authors.

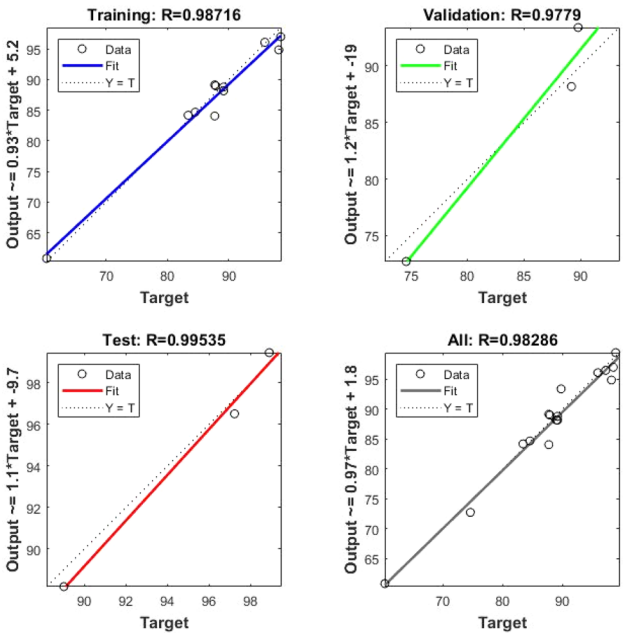

Fig. 11 Regression plot of the ANN model

Appendix

See Figs. 10, 11, 12, 13, 14 and 15.

Fig. 10 The ANN model

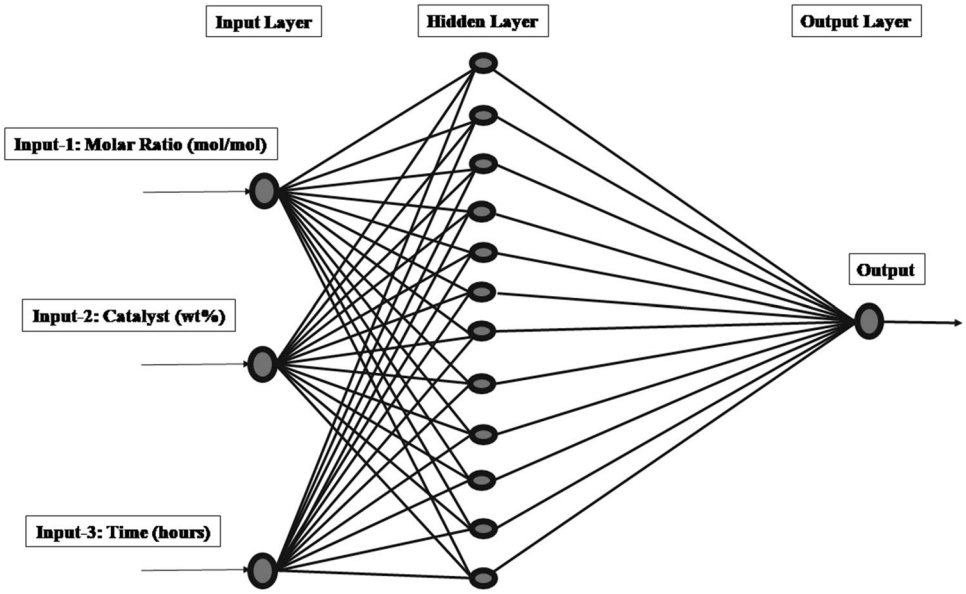

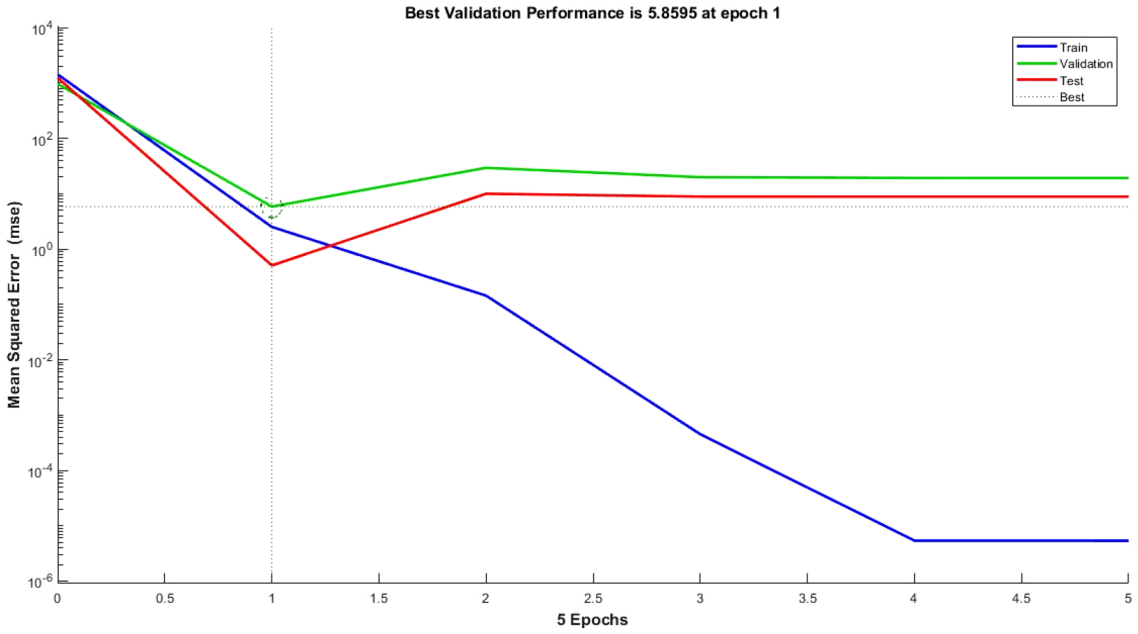

Fig. 12 Performance plot of the ANN model

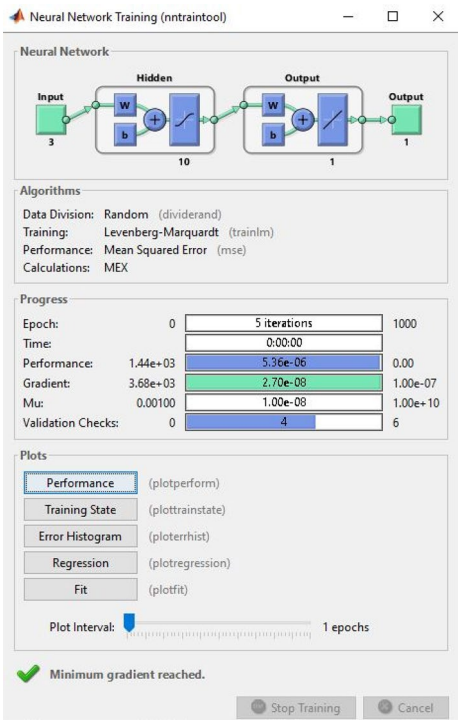

Fig. 13 Summary of ANN modeling

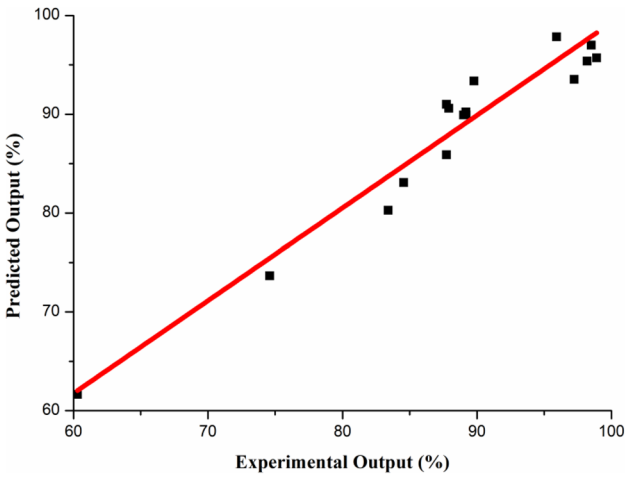

Fig. 14 Experimental output (%) vs predicted output (%) (RSM)

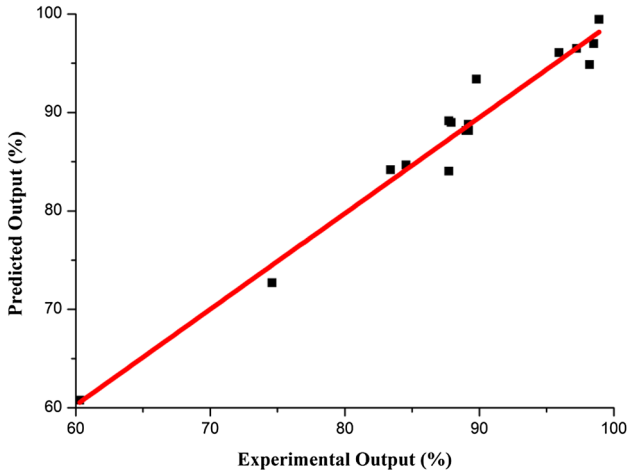

Fig. 15 Experimental output (%) vs predicted output (%) (ANN)

References

Ahmad H, Shahid A, Iqbal A, Jolius G, Muhammad HA (2016) Microwave reinforced transesterification of rubber seed oil using waste cement clinker catalyst. Curr Nanosci 12:1–10

Amish PV, Subrahmanyam N, Payal AP (2009) Production of biodiesel through transesterification of Jatropha oil using KNO_3/Al_2O_3 solid catalyst. Fuel 88:625–628

Anjana PA, Niju S, Begum KMMS, Anantharaman N, Anand R, Babu D (2016) Studies on biodiesel production from Pongamia oil using heterogeneous catalyst and its effect on diesel engine performance and emission characteristics. Biofuels 7:377. https://doi.org/10.1080/17597269.2015.1138039

Anuradha S, Joseph Antony Raj K, Vijayaraghavan VR, Viswanathan B (2014) Sulphated Fe_2O_3–TiO_2 catalysed transesterification of soybean oil to biodiesel. Indian J Chem A 53:1493–1499

Arpita G, Papita D, Keka S (2015) Modeling of biosorption of Cu(II) by alkali-modified spent tea leaves using response surface methodology (RSM) and artificialneural network (ANN). Appl Water Sci 5:191–199

Bharadwaj AVSL, Niju S, Begum KM, Anantharaman N (2019) Optimization and modeling of biodiesel production using fluorite as a heterogeneous catalyst. Energy Sources Part A Recov Util Environ Effects 41(15):1862–1878

Canan K, Candan H, Akin B, Osman A, Sait E, Abdurrahman S (2009) Methyl ester of peanut (*Arachis hypogea* L.) seed oil as a potential feedstock for biodiesel production. Renew Energy 34:1257–1260

Chandrasekaran M, Ramachandran P, Periyasamy N, Raghavan S, Govindasamy S, Manoj Kumar N (2017) Process optimization and kinetic modeling of biodiesel production using non-edible Madhuca indica oil. Fuel 195:217–225

Chouhan APS, Sarma AK (2011) Modern heterogeneous catalysts for biodiesel production: a comprehensive review. Renew Sustain Energy Rev 15:4378–4399

Cynthia OB, Lee KT (2013) The potential of using cocoa pod husks as green solid base catalysts for the transesterification of soybean oil into biodiesel: effects of biodiesel on engine performance. Chem Eng 220:395–401

da Costa Evangelista JP, Gondim AD, Di Souza L (2016) Alumina-supported potassium compounds as heterogeneous catalysts for biodiesel production: a review. Renew Sustain Energy Rev 59:887–894

Efavi JK, Dindomah K, Apalangya V, Nyankson E et al (2018) The effect of NaOH catalyst concentration and extraction time on the yield and properties of *Citrullus vulgaris* seed oil as a potential biodiesel feed stock. S Afr J Chem Eng 25:98–102

Ehsan M, Chowdhury MT (2015) Production of biodiesel using alkaline based catalysts from waste cooking oil: a case study. Proced Eng 105:638–645

Fadjar G, Shiro S (2015) Advanced supercritical methyl acetate method for biodiesel production from Pongamia pinnata oil. Renew Energy 83:1245–1249

Georgogianni KG, Katsoulidis AP, Pomonis PJ, Kontominas MG (2009) Transesterification of soybean frying oil to biodiesel using heterogeneous catalysts. Fuel Process Technol 90:671–676

Gerhard K (2001) Determining the blend level of mixtures of biodiesel with conventional diesel fuel by fiber-optic near-infrared spectroscopy and ^{1}H nuclear magnetic resonance spectroscopy. JAOCS 78:1025–1028

Girish N, Niju S, Begum KM, Anantharaman N (2013) Utilization of a cost effective solid catalyst derived from natural white bivalve clam shell for transesterification of waste frying oil. Fuel 111:653–658

Ikwuagwu OE, Ononogbu IC, Njoku OU (2000) Production of biodiesel using rubber [*Hevea brasiliensis* (*Kunth. Muell.*)] seed oil. Ind Crop Prod 12:57–62

Istadi I, Sebastianus AP, Tito SN (2015) Characterization of K_2O/CaO–ZnO catalyst for transesterification of soybean oil to biodiesel. Proced Environ Sci 23:394–399

Jaya N, Selvan BK, Vennison SJ (2015) Synthesis of biodiesel from pongamia oil using heterogeneous ion-exchange resin catalyst. Ecotoxicol Environ Saf 121:3–9

Jemaa M, Abbassi MA, Kamel G, Omri A, Jeguirim M (2015) Simulation of biofuel production via fast pyrolysis of palm oil residues. Fuel 159:819–827

Jilse S, Chandrasekharan M, Arockiasamy S (2016) A comparative study between chemical and enzymatic transesterification of high free fatty acid contained rubber seed oil for biodiesel production. Cogent Eng 3:1178370

Jolius G, Shahid A, Chitra Charan S, Charan K, Liyana Amer S, Nurul Hidayah MG, Chin KC, Said N (2012) Biodiesel production from rubber seed oil using a limestone based catalyst. AMPC 2:138–141

Junaid A, Suzana Y, Awais B, Ruzaimah N, Mohammad K (2014) Study of fuel properties of rubber seed oil-based biodiesel. Energy Convers Manag 78:266–275

Katarina M, Rajkovic JMA, Petar SM, Olivera SS, Vlada BV (2013) Optimization of ultrasound-assisted base-catalyzed methanolysis of sunflower oil using response surface and artificial neural network methodologies. Chem Eng J 215:82–89

Kumar Dipesh, Singh Bhaskar, Banerjee Ayan, Chatterjee Sandeep (2018) Cement wastes as transesterification catalysts for the production of biodiesel from Karanja oil. J Clean Prod 183:26–34

Leibbrandt NH, Aboyade AO, Johannes HK, Johann FG (2013) Process efficiency of biofuel production via gasification and Fischer–Tropsch synthesis. Fuel 109:484–492

Madhu A, Garima C, Chaurasia SP, Kailash S (2012) Study of catalytic behavior of KOH as homogeneous and heterogeneous catalyst for biodiesel production. J Taiwan Inst Chem E 43:89–94

Mahbub M, Kaniz F, Maksudur RK, Mazumder MSI, Islam MA, Uddin MT (2011) Rubber seed oil as a potential source for biodiesel production in Bangladesh. Fuel 90:2981–2986

Martin H, Frantisek S, Libor C, Michal C, Petr K (2012) Ethanolysis of rapeseed oil by KOH as homogeneous and as heterogeneous catalyst supported on alumina and CaO. Energy 48:392–397

Medeiros AM, Santos ERM, Azevedo SHG et al (2018) Chemical interesterification of cotton oil with methyl acetate assisted

by ultrasound for biodiesel production. Braz J Chem Eng 35(3):1005–1018
Melvin DFJ, Edwin Raj R, Durga Prasad B, Robert Kennedy Z, Mohammed Ibrahim A (2011) A multi-variant approach to optimize process parameters for biodiesel extraction from rubber seed oil. Appl Energy 88:2056–2063
Mostafa F, Nahid H, Nakisa Y, Rohollah E (2017) Preparation, characterization, kinetic and thermodynamic studies of MgO–La_2O_3 nanocatalysts for biodiesel production from sunflower oil. Chem Phys Lett 677:19–29
Mote VD, Purushotham Y, Dole BN (2012) Williamson–Hall analysis in estimation of lattice strain in nanometer-sized ZnO particles. JTAP 6:1–8
Niju S, Begum KMMS, Anantharaman N (2014a) Enhancement of biodiesel synthesis over highly active CaO derived from natural white bivalve clamshell. Arab J Chem 9:1–7
Niju S, Begum KMMS, Anantharaman N (2014b) Preparation of biodiesel from waste frying oil using a green and renewable solid catalyst derived from egg shell. Environ Prog Sustain Energy 34(1):248. https://doi.org/10.1002/ep.11939
Niju S, Niyas M, Begum KMMS, Anantharaman N (2014c) KF-impregnated clam shells for biodiesel production and its effect on a diesel engine performance and emission characteristics. Environ Prog Sustain Energy 34(4):1166. https://doi.org/10.1002/ep.12070
Obie F, Hasanah N, Matsumura Y (2015) Artificial neural network modeling to predict biodiesel production in supercritical methanol and ethanol using spiral reactor. Proced Environ Sci 28:214–223
Olubunmi OA, Folasegun AD (2014) Production of biodiesel from *Calophyllum inophyllum* oil using a cellulose-derived catalyst. Biomass Bioenergy 70:239–248
Olusegun DS, Modestus OO (2018) Comparison of response surface methodology (RSM) and artificial neural network (ANN) in modelling of waste coconut oil ethyl esters production. Energy Source Part A Recov Util Environ Effects. https://doi.org/10.1080/15567036.2018.1539138
Pisitpong I, Sotsanan I, Apanee L, Samai JI (2014) Biodiesel production from palm oil using potassium hydroxide loaded on ZrO_2 catalyst in a batch reactor. Chiang Mai J Sci 41(1):128–137
Poonam Singh N, Anoop S (2011) Production of liquid biofuels from renewable resources. Prog Energy Combust Sci 37:52–68
Prabu A, Anand RB (2015) Inhibition of NO emission by adding antioxidant mixture in *Jatropha* biodiesel on the performance and emission characteristics of a CI engine. Front Energy 9(2):238–245
Qing S, Bolun Y, Hong Y, Song Q, Gangli Z (2007) Synthesis of biodiesel from soybean oil and methanol catalyzed by zeolite beta modified with La^{3+}. Catal Commun 8:2159–2165
Ramadhas AS, Jayaraj S, Muraleedharan C (2005) Biodiesel production from high FFA rubber seed oil. Fuel 84:335–340
Ru Y, Mengxing S, Jianchun Z, Fuqiang J, Chunhong Z, Min L, Xinmin H (2011) Biodiesel production from rubber seed oil using poly (sodium acrylate) supporting NaOH as a water-resistant catalyst. Bioresour Technol 102:2665–2671
Sakdasri W, Sawangkeaw R, Ngamprasertsith S (2017) An entirely renewable biofuel production from used palm oil with supercritical ethanol at low molar ratio. Braz J Chem Eng 34(4):1023–1034
Satyanarayana M, Muraleedharan C (2010) Methylester production from rubber seed oil using two step pretreatment process. Int J Green Energy 7:84–90
Sirajuddin M, Tariq M, Ali S (2015) Organotin(IV) carboxylates as an effective catalyst for the conversion of corn oil into biodiesel. J Organomet Chem 779:30–38
Sneha EM, Anand R, Begum KMMS, Anantharaman N (2015) Biodiesel production from waste cooking oil using KBr impregnated CaO as catalyst. Energy Convers Manag 91:442–450
Sunil D, Bhushan G, Kashyap KD (2013) Development of a combined approach for improvement and optimization of karanja biodiesel using response surface methodology and genetic algorithm. Front Energy 7(4):495–505
Surbhi S, Ajay KA, Rajendra PB, Deepak KT (2011) Biodiesel production using heterogeneous catalysts. Bioresour Technol 102:2151–2161
Syazwani ON, Hwa ST, Aminul I, Taufiq-Yap YH (2017) Transesterification activity and characterization of natural CaO derived from waste venus clam (*Tapes belcheri* S.) material for enhancement of biodiesel production. Process Saf Environ 105:303–315
Taufiq-Yap YH, Lee HV, Yunus R, Juan JC (2011) Transesterification of non-edible *Jatropha curcas* oil to biodiesel using binary Ca–Mg mixed oxide catalyst: effect of stoichiometric composition. Chem Eng 178:342–347
Thodinh SV, Trung NP, Vu Nguyen A, Huong Nguyen L, Anh TK (2016) Optimization of esterification of fatty acid rubber seed oil for methyl ester synthesis in a plug flow reactor. Int J Green Energy 13(7):720–729
Trisupakitti S, Ketwong C, Senajuk W, Phukapak C, Wiriyaumpaiwong S (2018) Golden apple cherry snail shells catalyst for heterogeneous transesterification of biodiesel. Braz J Chem Eng 35(4):1283–1291
van der Westhuizen I, Walter WF (2018) Stabilizing sunflower biodiesel with synthetic antioxidant blends. Fuel 219:126–131
Vipin VC, Sebastian J, Muraleedharan C, Santhiagu A (2016) Enzymatic transesterification of rubber seed oil using *Rhizopus oryzae* lipase. Proced Technol 25:1014–1021
Wang K, Jiang J, Zhan S, Liang X (2013) Biodiesel production from waste cooking oil catalyzed by solid acid $SO_4^{2-}/TiO_2/La^{3+}$. J Renew Sustain Energy 5:052001. https://doi.org/10.1063/1.4820563
Wei X, Jiwu X, Lijing G, Guomin X (2015) Preparation and characterization of inorganic acid catalytic membrane for biodiesel production from oleic acid. Asia Pac J Chem Eng 10:851–857
Wenlei X, Dong Y (2012) Transesterification of soybean oil over WO_3 supported on $AlPO_4$ as a solid acid catalyst. Bioresour Technol 119:60–65
Wenlei X, Haitao L (2006) Alumina-supported potassium iodide as a heterogeneous catalyst for biodiesel production from soybean oil. J Mol Catal A Chem 255:1–9
Wenlei X, Liangliang Z (2013) Production of biodiesel by transesterification of soybean oil using calcium supported tin oxides as heterogeneous catalysts. Energy Convers Manag 76:55–62
Wenlei X, Xiaoming H, Haitao L (2007) Soybean oil methyl esters preparation using NaX zeolites loaded with KOH as a heterogeneous catalyst. Bioresour Technol 98:936–939
Wuttichai R, Theeranun S, Boonyawan Y, Taweesak S, Vinich P (2017) Rubber seed oil as potential non-edible feedstock for biodiesel production using heterogeneous catalyst in Thailand. Renew Energy 101:937–944
Yong-Ming D, Jhong-Syuan W, Chiing-Chang C, Kung-Tung C (2015) Evaluating the optimum operating parameters on transesterification reaction for biodiesel production over a $LiAlO_2$ catalyst. Chem Eng 280:370–376
Zamberi MM, Ani FN (2016) Biodiesel production from high FFA rubber seed oil using waste cockles. ARPN J Eng Appl Sci 11(12):7782–7787

Affiliations

Sai Bharadwaj Aryasomayajula Venkata Satya Lakshmi[1] · Niju Subramania Pillai[2] · Meera Sheriffa Begum Khadhar Mohamed[1] · Anantharaman Narayanan[1]

[1] Department of Chemical Engineering, National Institute of Technology-Tiruchirappalli, Tiruchirappalli, Tamilnadu 620015, India

[2] Department of Biotechnology, PSG College of Technology, Coimbatore, Tamilnadu, India